Relating Nanoindentation to Macroindentation of Wood

Robert J. Moon[1*], Joseph E. Jakes[1], Jim F. Beecher[1], Charles R. Frihart[1] and Donald S. Stone[2]

[1]USDA Forest Service, Forest Products Laboratory, One Gifford Pinchot Drive, Madison, WI 53726, USA
[2]Department of Materials Science and Engineering, University of Wisconsin-Madison
1509 University Ave. Madison, WI 53706, USA

Abstract

Wood has several levels of hierarchical structure, spanning from the configuration of growth-rings down to the configuration of the base polymers (cellulose, hemicellulose, and lignin). The bulk properties of wood result from the culmination of interactions over all length scales. Gaps presently exist in the fundamental knowledge relating the contribution of wood properties at each structural level to the resulting bulk properties. The advent of nanoindentation has facilitated mechanical property measurement at the cell wall layer; however, there is limited understanding of how and to what extent the properties at the cell wall level influence the bulk properties.

This paper summarizes some preliminary work relating hardness measurement by nanoindentation to macroindentation. Nanoindentation was used to measure hardness within the cell wall S2 layer of radiata pine *(Pinus radiata)* latewood (LW) cells, whereas macroindentation was used to indent the same LW band from which the nanoindentation specimens were obtained. Meyer hardness measured via nanoindentation was found to be ~5 times larger than that measured by macroindentation. The differences in measured hardness between the two scales of indentation has been consider to result from differences in woody material volume fraction and the structure of the material being deformed. Additionally, the effects of a wood chemical modification treatment on the measured hardness for nanoindentation and macroindentation hardness demonstrated how changes in cell wall latewood properties propagate though to bulk hardness measurements of latewood.

Introduction

For further advancement of wood chemical treatments there is a need to understand the mechanism of wood property modification at the microscopic level and relate this to changes in bulk wood properties and performance. Additionally, considering interactions between chemical modifications with the hierarchical structure of wood may offer opportunities for further bulk property improvements. Bulk material properties of hierarchical structured solids are directly affected by the structural hierarchy (Lakes, 1993).

For example, laminated fiber-reinforced matrix composites have two levels of hierarchical structure. The first structural level is within a single lamina, which has properties that result from the reinforcement-matrix structure and its interfacial properties and the properties of each material. The second structural level results from the stacking sequence of each lamina where the fiber orientation within each lamina is systematically varied. The bulk composite properties are based on the response from both levels of structure. A similar effect occurs in natural structures (bone, wood, and plants) though there are several more structural levels.

The unique properties of wood are a direct result of wood's hierarchical structure. The structure of wood spans many length scales (Fig. 1): meters for describing the whole tree, centimeters for describing structures within the tree cross section (pith, heartwood, sapwood, and bark), millimeters for describing growth rings (earlywood, latewood), micrometers for describing different wood tissues (tracheids), and the layer structure within cell walls (primary, S1, S2, and S3), nanometers for describing the configuration of cellulose-fibrils in a matrix of hemicellulose and lignin, and the sub-nanometer scale for describing the molecular structures of cellulose, hemicellulose, and lignin and their chemical interactions. The bulk properties of wood are considered to be influenced by six general structural levels, corresponding to a unique set of identifiable features or structures. Note that the properties of larger features are influenced by the properties of all lower size features. For example, bulk wood properties are effectively based on growth ring properties and their relative configuration, which are based on earlywood (EW) and latewood (LW) properties, which are based on wood cell properties, which are based on cell wall properties, which are based on fibril-matrix properties within each cell wall layer, which are based on properties of cellulose, hemicellulose, and lignin domains. The challenge has been to understand the role of each structural level on bulk properties.

Extensive research has been conducted on structure–propertyrelationships investigating wood dimensional stability and elastic properties (Kelsey, 1963; Neagu et al., 2006; Pang, 2002) and wood compression strengths (Gindl and Teischinger, 2002). Most studies on hierarchal structural effects have typically considered two or three levels of structure: relating ultrastructural (cellulose fibrils in a matrix of lignin and hemicelulose) to preparation of a single cell wall layer, which are related to the multilayered, multicell wall properties and then to properties of a single wood cell (Bergander and Salmen, 2002; Neagu et al., 2006). Studies investigating additional levels of hierarchal structure have used multi-level homogenizations schemes where each level accounts for a particular structure (hemicellulose-lignin effective properties, cellulose-fibrils in matrix, wood cellular structure) to model bulk material properties (Hofstetter et al., 2005). These studies have advanced the fundamental knowledge regarding the contribution of each wood structural level on resulting bulk properties. In particular, laminate theory has been effective in modeling wood cell wall structure, accounting for fibril-matrix ultrastructure within each layer and layer stacking of the cell wall. However, there is a need to provide experimental confirmation of these models and their contribution to the bulk properties of wood.

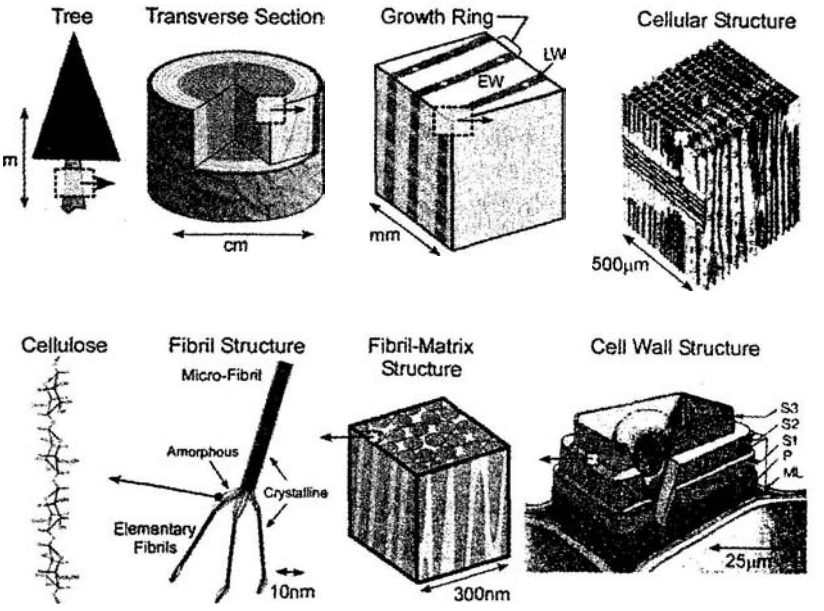

Fig.1. Hierarchical structure of wood. Six levels of structure influence bulk properties: Growth ring, earlywood and latewood, cellular structure, layer structure of cell wall, fibril-matrix structure, and the structure/configuration of the main polymer components (cellulose, hemicelluse, and lignin).

The advent of nanoindentation has facilitated mechanical property measurement at the cell wall layer (Jakes, 2007; Moon et al., 2006; Tze et al., 2007). Nanoindentation has been used to investigate ultrastructural effects on measured hardness and elastic modulus as a function of cellulose fibril angle (Gindl and Schöberl, 2004; Gindl et al., 2004; Tze et al., 2007), lignin content (Gindl et al., 2002; Gindl et al., 2004), extractive content (Tze et al., 2007), growth ring location (Tze et al., 2007), earlywood vs. latewood (Wimmer et al., 1997), and chemical modification (Gindl and Gupta, 2002; Gindl et al., 2004). The cell wall longitudinal elastic modulus as measured by nanoindentation was different from that predicted by laminate theory (Gindl and Schoberl, 2004; Tze et al., 2007) and is less than half of that measured by the tensile modulus of single wood fibers (Gindl and Schoberl, 2004). The origins of these disparities can be attributed to inaccuracies in model input variables (material properties, fibril stackmg and orientation, boundary conditions), differences in loading conditions (in model and in experiments), the nanoindentation technique employed, and the contribution of material anisotropy. The challenges for wood modification research will be to address the above-mentioned disparities and then relate changes in cell wall modulus caused by chemical treatment to changes in the modulus of bulk wood.

The complex nature of permanent deformation of hierarchical structures has hindered systematic investigations (experimental testing and modeling) comparing the deformation modes of nanoindentation and macroindentation. However, experiments have shown that the change in hardness as a function of cellulose-fibril angle follows a similar relationship for nanoindentation of cell walls to macroindentation of bulk wood (Holmberg, 2000; Tze et al., 2007). This suggests a possibility of relating changes in measured hardness at the cell wall layer to the hardness of bulk wood. If this mechanism can be understood, it may

offer a new technique for investigating wood chemical treatments targeting particular wood cell wall modification. Additionally, for development of better predictive models for wood hardening applications, we need to develop an understanding of the relative contribution of each hierarchical level of structure to bulk deformation properties and to identify experimental techniques that can be used to do this.

This paper summarizes preliminary work comparing cell wall hardness of individual LW cells (as measured by nanoindentation) to the macroscopic hardness measurement of the same LW band. Additionally, a bio-based wood chemical modification treatment was used to evaluate how changes in hardness within the cell wall coincide with changes in hardness within LW bands. The ultimate aim of this research is to understand the mechanism of property change at the micron and submicron level and correlate this to the mechanism that changes the bulk properties and performance.

Indentation of Homogeneous Structured Solids

Indentation techniques have been widely used for measuring mechanical properties of materials because of the ease and speed of conducting the tests. The basic premise of all indentation techniques is that an indenter (e.g., hard material of specified shape) is pressed into the surface of a softer material with sufficient force that the softer material deforms. The measured properties are based on the deformation response of the softer material. The volume of deformed material beneath the indenter (interaction volume) is assumed to have homogeneous structure and properties, and the resultant mechanical properties describe the average deformation response. Deformation can occur by several modes: elastic, viscoelastic, plastic, creep, and fracture. These deformation modes are described respectively by the following properties: elastic modulus, relaxation modulus, hardness, creep rate, and fracture toughness. By modifling the applied load and/or the indenter size and shape, the interaction volume size can be modified. When the interaction volume is decreased, mechanical properties of smaller sized features can be measured. Fig. 2 shows the approximate range of feature sizes that can be measured for macroindentation, microindentation, nanoindentation, and atomic force microscopy (AFM).

A phenomenon that complicates property comparisons between indentation techniques is indentation size effect (ISE), for which there is an increase of hardness with decreasing indention size or indentation depth (Manika and Maniks, 2006; Tze et al., 2007). ISE is not well understood but has been widely studied for metals, ceramic, and polymers, resulting in several mechanisms that may account for its occurrence: surface effects, strain gradient effects, changing elastic-plastic deformation contribution, friction between the indenter and the specimen, and structural non-uniformity of the deformed area. For wood, the concept of ISE is more complicated and may be inappropriate because as the indentation size increases there may be large changes in wood structure within the interaction volume, which will dominate the deformation response. However, when indenting on similarly structured materials, such as nanoindentation of the wood cell wall S2 layer, ISE has been shown to be relatively small (Jakes et al., 2007; Tze et al., 2007).

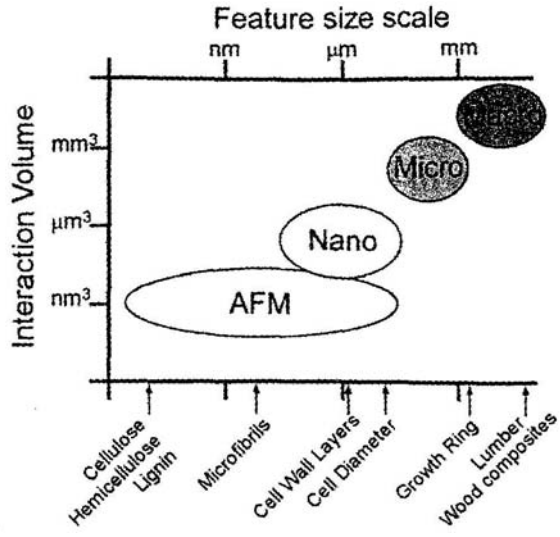

Fig. 2. The size scale of atomic force microscopy (AFM), nano, micro, and macroindentation related to the wood structural scale.

Indentation of Hierarchical Structured Solids

Indentation techniques offer an approach for investigating mechanical properties at several structural levels. Solids with internal structures (grain size, layers, composition variations) require additional consideration as to the effect of the structure on uniformity of the interaction volume. The interaction volume needs to be appropriately scaled to the structural feature of interest. By using an interaction volume smaller than the feature, the properties of that feature can be measured, whereas by increasing the interaction volume to several times the feature size, the specific contribution of that feature to the bulk deformation response may be identified. However, if the interaction volume is between these extremes, artifacts may be induced by structural variability within the interaction volume. For example, when investigating effects of growth ring orientation on hardness, the interaction volume should include several growth rings to minimize artifacts associated with changes in volume fraction of EW and LW within the interaction volume for each indent, regardless of growth ring orientation.

Macroindentation is considered in this study for indentations greater than 1 mm. The Janka hardness technique (ASTM, 2085; Green et al., 2006), having an 11.3-mm-diameter sphere indenter, was developed for measuring bulk wood hardness, in which the interaction volume includes several growth rings. Several macroindentation investigations have shown the influence of different material parameters on wood bulk hardness, such as wood species, density, moisture content, wood structural orientation (radial, tangential, transverse), and grain direction (Doyle and Walker, 1985; Green et al., 2006; Holmberg, 2000). For fine-grained wood, the interaction volume has similar EW/LW ratio between indents, and a more consistent bulk hardness measurement can be achieved. However, for wide-grained wood typical of plantation-grown trees, there is increased variability of the EW/LW ratio within the interaction volume, resulting in a large distribution on measured hardness based on indentation location.

Smaller indenter sizes have been used to measure hardness variation across single growth rings (Hirata et al., 2001), where the growth ring contribution is removed (Fig. 3a). The interaction volume encompasses many wood cells of a more consistent wood structure (all cells are EW or LW). The higher hardness of LW compared with EW can primarily be attributed to higher wood density (increased volume fraction of cell wall material to lumen as shown in Fig. 3a). The hardness of LW has been shown to be 2 to 10 times larger than EW and is dependent on wood species and wood structural orientation (Hirata et al., 2001).

Microindentation (e.g., Vickers and Knoop) typically uses small pyramidal-shaped indenters that have corresponding indent sizes of 30 to 1000 μm. However, the corresponding interaction volume size is similar to the transverse wood cell size, and great care is needed to ensure a homogeneous structure within the interaction volume. For example, when indenting on transverse cell wall sections, the indent should be several times larger than the cell size. Otherwise, a vastly different deformation response will occur if the indenter tip lands in the center of a lumen rather than the cell wall. For the current study, microindentation was not completed because the size of the interaction volume did not scale well with the wood cell structure investigated.

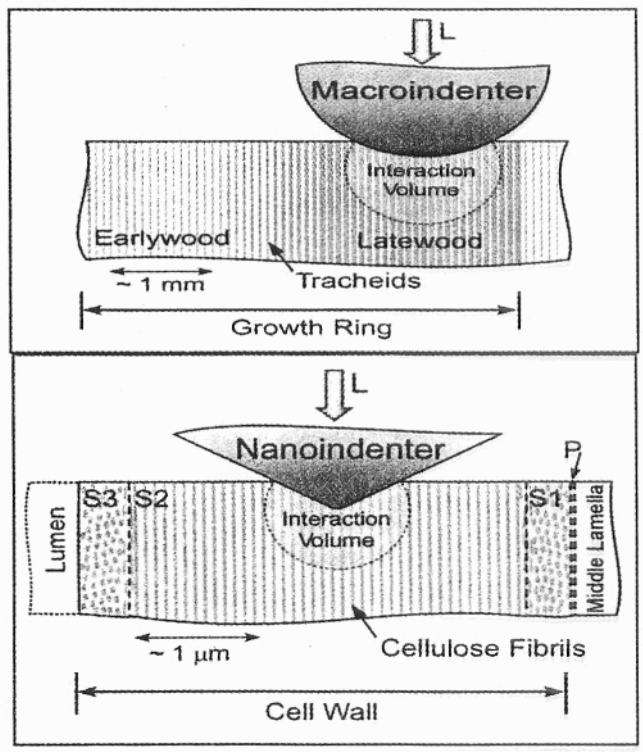

Fig. 3. The corresponding interaction volume related to the wood structure for a) macroindentation of latewood band (cellular structure), and b) nanoindentation of the S2 layer within the a tracheid cell wall (fibril–matrixstructure). Indentation is parallel to the longitudinal axis.

Nanoindentation, also referred to as depth-sensing indentation, uses much smaller indenters and applied loads resulting in a much smaller interaction volume, which allows the mechanical properties of much finer features to be measured. For wood-based materials, the interaction volume is sufficiently small that mechanical properties within cell walls, in

particular the S2 and middle lamella, can be measured. This allows the deformation response of cellulose-fibrils in a matrix of hemicellulose and lignin to be investigated (Fig. 3b). This type of mechanical-properties measurement provides information about wood cell-wall properties. Unlike other indentation techniques, there is currently no direct applicability of this measurement technique to deformation of bulk wood.

Experimental Procedures

Specimen Preparation

Plantation-grown radiata pine *(Pinus radiata)* with a growth-ring spacing of 10 to 20 mm was used in this study. The average LW band was - 3 to 5 mm wide, whereas the combined EW and transition wood bands were ~ 7 to 15 mm wide. The wood was preconditioned at 24°C and 65% relative humidity. Macroindentation tests were completed on the transverse surface having a surface roughness that resulted from the cut. In addition to untreated material, testing was also conducted on radiata pine that was chemically modified by a proprietary starch-based wood-hardening treatment.

Nanoindentation requires ultra-smooth surfaces free from surface preparation artifacts. A gently sloping apex was microtomed on the transverse surface of a wood cube such that the apex was positioned in the LW band (Fig. 4). A sledge microtome fit with a custom-built diamond knife holder was used to cut the tip of the apex. The result was an exceptionally smooth surface having an area of ~0.5 mm^2. Best results were achieved when the clearance angle and cutting angle were both set to approximately 5°. This surface preparation technique did not require specimen embedment, eliminating the possibility of cell wall chemical modification by the embedment medium. Note that only smooth surfaces were produced for latewood specimens. The specimen base was bonded to a 1-cm diameter steel disk that could be magnetically clamped to the nanoindenter specimen stage.

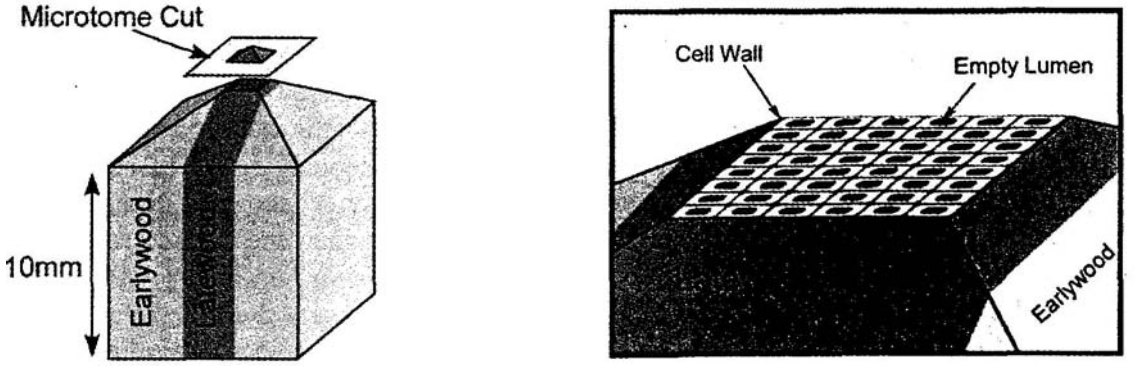

Fig. 4. Schematic showing a) specimen configuration for surfaces produced by microtoming un-embedded wood, b) higher magnification of representative smooth surface having empty lumina.

All indention tests were completed on transverse sections, where the measured hardness from macroindentation and nanoindentation were completed on the same LW band.

Macroindentation Measurements:

Macroindentation was completed with a spherical indenter having a diameter of D = 3.18 mm. The fixture was attached to an Instron™ (Model 5566, Norwood, MA, USA) testing machine. Load was measured using a calibrated load cell having a maximum range of 8900 N. The machine crosshead movement, having precision to nearest 0.0024 mm was used to measure the indenter displacement. The load was applied continuously throughout the test at a uniform rate of 6 mm/min. The load, L, and indentation displacement, h, were continuously recorded at a rate of 50/s, and test was completed at displacement slightly greater than D/2. The Meyer hardness was calculated for two different indenter depths: 0.5 mm and D/2. Both have sufficient indentation depth to minimize surface roughness artifacts.

Meyer hardness, H_M, is the ratio of applied force to the projected contact area, A_{proj}, and was calculated using the following equations.

$$H_M = \frac{L}{A_{proj}} = \frac{4L}{\pi d^2} \quad \text{(MPa)} \tag{1}$$

$$d = 2\sqrt{\left(\left(\frac{D}{2}\right)^2 - \left(\frac{D}{2} - h\right)^2\right)} \quad \text{(mm)} \tag{2}$$

where d is the impression diameter for a given indentation depth, and for 0.5 mm indenter depth, Equation (2) was used to calculate the indenter diameter. For the D/2 indentation depth, the indent diameter was measured using digital images of the surface, in which the average indent diameter from two orthogonal measurements of the indent were used.

Nanoindentation Measurements:

A Hysitron (Minneapolis, MN, USA) Triboindenter® equipped with a diamond Berkovich tip (~100 nm tip radius) was used in this study. A force-control loading sequence was used for all indentations: a 5-second ramp up to 400 μN applied load, a 5-second hold, and then a 5-second ramp down. During the nanoindentation process, the applied load and indenter displacement were simultaneously recorded as the indenter is driven into and withdrawn from a material. As part of standard Hysitron procedure, thermal drift was also calculated by holding the tip against the surface at 1 μN load and recording the displacement for 300 seconds prior to making an indent. A linear fit to the data from the last 50 seconds of this hold was used to measure thermal drift.

During unloading, surface displacements perpendicular to the loading direction are negligible (Sakai and Nakano, 2002); therefore, residual indent areas can be considered equivalent to contact areas during maximum load. The projected indent area, A_{proj}, was measured from images taken by a Quesant (Agoura Hills, CA, USA) AFM that was attached to the same loading frame as the nanoindenter. The AFM was operated in contact mode and was calibrated using an Advanced Surface Microscopy Inc.[a] (Indianapolis, IN USA) calibration standard with a pitch of 292 ± 0.5 nm. Successive 4 μm scans and

[a] www.asmicro.com

calibration routines revealed the reproducibility of the AFM calibration was ±1%. Individual 4 μm by 4 μm scans of each indent for both z-height and lateral force measurements were used to manually measure the projected indent areas using ImageJ[a] image analysis software. The areas were measured by carefully outlining the edges of contact as illustrated in Fig. 5.

Nanoindentation was used to calculate the Meyer hardness, H_{nM},

$$H_{nM} = \frac{L_{\max}}{A_{proj}} \quad \text{(MPa)} \qquad (3)$$

where L_{max} is the load at maximum depth.

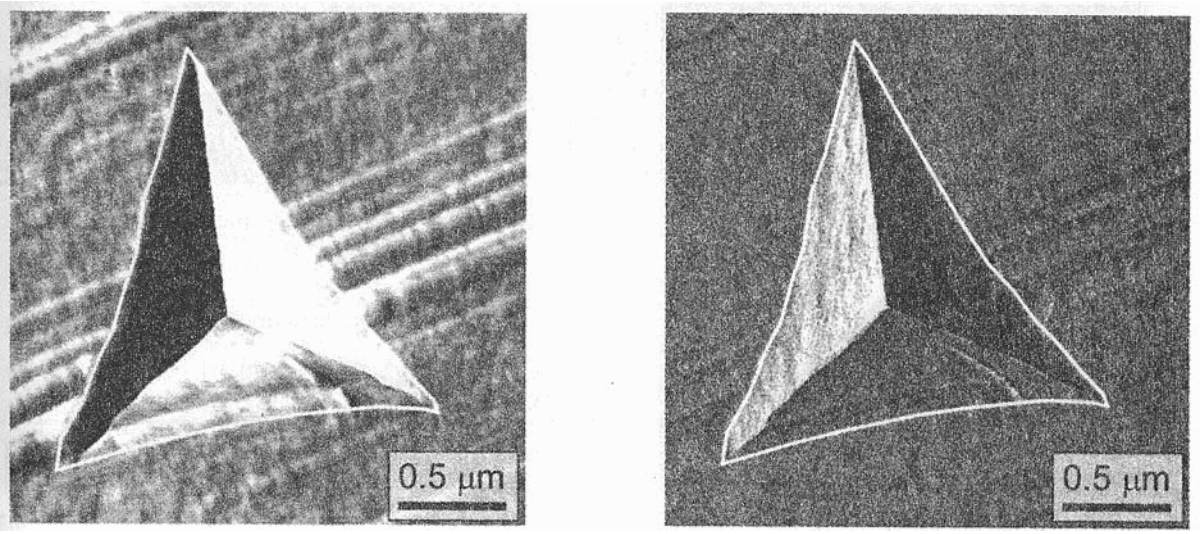

Fig. 5. Atomic force microscopy (AFM) images of an indent in a tracheid wall (S2 layer), both a) lateral force and b) z-height images are used to conjunction to confirm indent contact areas. Note the outline shows the contact area that was used for this indent.

Results and Discussion

Hardness Measurement

Nanoindentation was completed on the LW cell wall S2 layer as shown in Fig. 6, for untreated and treated radiata pine, respectively. Indents within the S2 cell wall layer were used for analysis. Variations of the indent shape on measured hardness were accounted for as indent areas were individually measured rather than calculated from indentation depth. Nanoindentation hardness for untreated radiata pine (URP) was 358 MPa and 387 MPa for treated radiata pine (TRP, Table I). These hardness values are within the range that has been measured for other wood species using nanoindentation (Gindl et al., 2002; Gindl and Gupta, 2002; Gindl et al., 2004; Jakes et al., 2007; Jakes, 2007; Tze et al., 2007). Note that

[a] hm://rsb.info.nih.gov/ij/

LW specimens of URP and TRP came from different trees and the differences in hardness between the two may not necessarily be a result of the treatment process. Subsequent studies will investigate URP and TRP from the same growth rings.

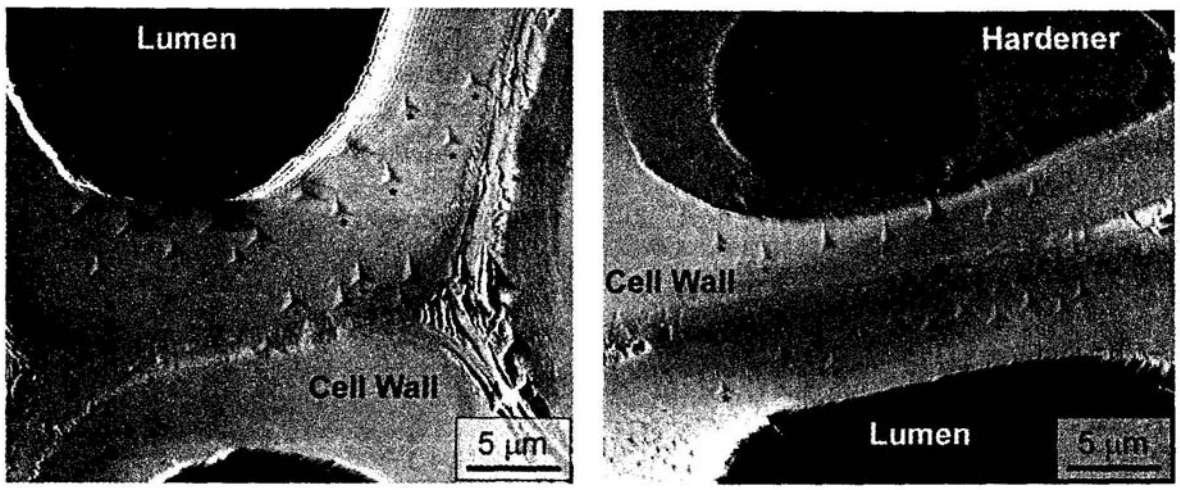

Fig. 6. Atomic Force images of a) untreated radiata pine and b) treated radiata pine after nanoindentation. Indents mark with astericks were used in the analysis.

Table 1. Latewood hardness measured by nanoindentation.

Treatment	Number of indents	Meyer hardness (MPA)	Standard deviation	Growth ring
Untreated				
Nanoindentation	12	358	30	a
Macroindentation				
0.5mm depth*	7	66	1	a
D/2 depth**		67	2	
Treated				
Nanoindentation	14	387	23	b
Macroindentation				
0.5mm depth*	7	87	12	b
D/2 depth**		94	2	

* calculated contact diameter
**measured contact diameter

Macroindentation was completed on the same LW band from which the nanoindentation specimens were obtained. Fig. 7 shows a typical indent within the LW band, after D/2 indentation depth, of untreated and treated radiata pine. The effective contact diameter for the 0.5 mm indentation depth was 2.32 mm, whereas the average measured contact diameter for the *D/2* indentation depths were URP = 3.05 mm and TRP = 2.92 mm. The importance of measuring the contact area is demonstrated for the *D/2* indentation depths, in which the estimated contact diameter calculated from Equation 2 would have been 3.18 mm and would have resulted in artificially low calculated hardness.

Since the contact area at both indentation depths was smaller than the typical LW band widths, the resulting interaction volume will have a uniform structure and the measured properties will be representative of that structure. The average hardness from the 0.5 mm indentation depth was URP = 66 MPa and TRP = 87 MPa (Table I). For *D/2* indentation depths, the calculated hardness was URP = 67 MPa and TRP = 94 MPa. Difference between the two indentation depths may have resulted from inaccuracies of contact diameter calculated for 0.5 mm indention depth (as a result of load-frame compliance, etc.) and from errors in the measured contact diameter for the *D/2* indentation depths. Note that for the indentation depth and applied load ranges used for macroindentation (500-700 N), 0.1-mm error in measured contact diameter corresponds to an error of ~6 MPa in hardness.

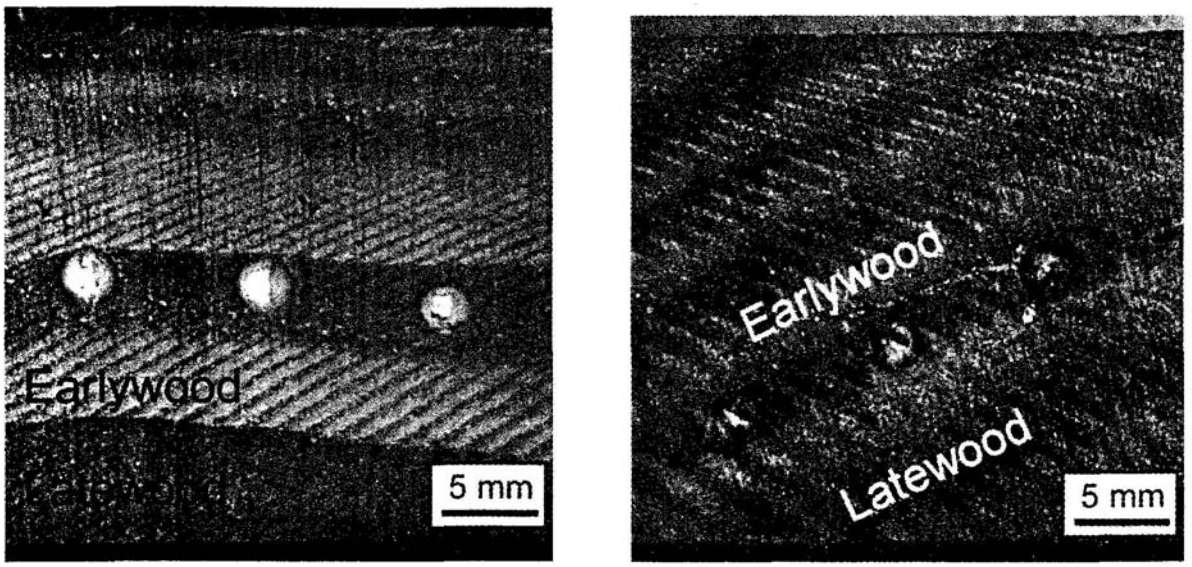

Fig. 7. Optical images of final indent impressions of 3.18 mm ball indenter within the latewood band of a) untreated radiata pine b) treated radiata pine. Note that the entire indent is within the latewood band with little contribution of transition wood.

Nanoindentation vs Macroindentation:

The hardness measured by macroindentation was ~20% of that measured by nanoindentation (Table I). The large deviation in measured hardness can be associated with difference in deformation response within the corresponding interaction volumes of macroindentation and nanoindentation (Fig. 3). Both indentation tests were completed in the longitudinal direction and on the same LW band; therefore, minimizing differences in grain orientation, cellulose micro-fibril angle, and extractive content. Any small changes in these factors would not have resulted in a large hardness difference between the two techniques (Tze et al., 2007). The differences in deformation response are considered to result from differences in the material density and the structure within the interaction volume.

The interaction volume for nanoindentation is the cell wall material comprised of cellulose, hemicellulose, and lignin and has a fiber-matrix structure (Fig. 3a). In contrast, the interaction volume for macroindentation is composed of several hundred wood cells, and because of the cellular structure of wood cells (i.e., open pore structure of the lumen),

there is a lower material density. It is reasonable to expect that the lower material density within the macroindentation interaction volume, as compared with nanoindentation, results in less woody material to resist deformation and results in lower measured hardness. This would be consistent with studies that have investigated the effects of wood density on properties, in which lower wood density has been shown to decrease bulk wood mechanical properties, hardness (Green et al., 2006; Holmberg, 2000), and compression strength (Gindl and Teischinger, 2002). Additionally, indentation studies in other material systems have shown that increased porosity results in much lower measured properties (Ferranti et al., 2004; Jang and Matsubara, 2005; Khor et al., 2003). Interestingly, one wood hardening mechanism used in industry is to fill wood cell lumen with a hardener resin, which effectively increases the amount of material to resist deformation. This mechanism has been used to more than double wood hardness (Ibach and Ellis, 2005).

Based on the above discussion, one contributing factor in the difference in measured hardness between nanoindentation and macroindentation is a result of the differences in woody material volume fraction within the indentation interaction volume. The contribution of the woody material volume fraction on hardness may be estimated by normalizing density within the interaction volume to the density of cell wall material according to Equation 4,

$$H_M = \frac{\rho}{1.5} H_{nM} \tag{4}$$

where 1.5 g/cm^3 is density of the cell wall material (Kelloge et al., 1975) and ρ is density of the material within the macroindentation interaction volume and was measured for LW to be URP = ~0.62g/cm^3 and TRP = ~0.66g/cm^3. The estimated macroscopic hardness for completely dense woody material was then calculated using nanoindentation hardness, Equation 4 and the respective UPR and TRP densities. The resulting estimated macroscopic hardness was URP = 148 MPa and TRP = 160M Pa, which is nearly twice that measured by macroindentation but still demonstrates that woody material volume fraction has a large contribution to measured hardness. The difference between estimated and measured macroscopic hardness may then be attributed to differences in structure within the interaction volume.

There are considerable differences in structure within the interaction volumes for macroindentation and nanoindentation, which will dictate deformation response. However, the specific effect of these structures on deformation is not currently well understood. The deformation mechanism during nanoindentation would likely occur preferentially by shear deformation along the weak fibril-matrix interface where hydrogen bonding connects the cellulose fibrils to the hemicellulose and lignin matrix.

In contrast, the macroindentation of wood cellular structures has additional deformation mechanisms: shear deformation across cell walls, shear deformation between wood cells along the middle lamella, and crushing or bowing of wood cell structure. The dominant deformation mechanism is difficult to assess as it is likely to be different during initial deformation vs. “steady-state” deformation. Compression tests of wood specimens along the axial direction have shown that initial deformation of wood cells occurs by localized

shear deformation within the cell wall (Gindl and Teischinger, 2002), in which compressive strength of wood is dictated by the shear yield strength of the composite cell wall. Subsequent deformation was dominated by crushing of the cells. For macroindentation, having a large component of compressive loading within its interaction volume, initial deformation might be strongly related to cell wall shear yield strength, whereas subsequent deformation is related to cell crushing. This suggests that by understanding cell wall deformation, we can gain insight into the initiation mechanism of macroscopic deformation. For permanent deformation, nanoindentation may be related to macroindentation based on the deformation response of cell wall material. This may partially explain a similar relationship exists for nanoindentation and macroindentation of hardness as a function of cellulose-fibril angle (Holmberg, 2000; Tze et al., 2007). This discussion suggests that nanoindentation may be used to investigate cell wall deformation response, and this may be related to at least one deformation mechanism in macroindentation.

Untreated vs. Treated Radiata Pine

For this preliminary study, only general comparisons can be made between URP and TRP specimens because the LW bands measured were different, and the exact contribution of the chemical treatment cannot be assessed. Indentation results were consistent in that there were increases in both nanoindentation (~8%) and macroindentation hardness (~32%) for the TRP as compared with URP. What the true mechanism was for this increase in macroindentation hardness is unclear, but it may have resulted from changes in cell wall chemistry (natural or via chemical treatment) or by changes in material density in the interaction volume (natural or via chemical treatment). Nanoindentation demonstrates an increased resistance to cell wall deformation; its contribution to the 32% increase in macroindentation hardness is unclear. The TRP LW band had a higher density (0.66 g/cm^3) compared with the URP LW band (0.62 g/cm^3). Fig. 6b shows partial filling of a lumen by the hardener resin, demonstrating that this is a contributing mechanism for the increase in material density within the interaction volume and would have contributed to the increase in the macroindentation hardness. Since the indent-projected contact areas were measured directly, the filled lumenia would not have influenced the nanoindentation hardness measurements. Interestingly, this relatively small change in density would not likely cause such a large change in macroscopic hardness (Green et al., 2006; Holmberg, 2000), suggesting a different dominant hardening mechanism. It is unclear at this point whether cell wall modification is the dominant mechanism; however, this comparison effectively demonstrates that for chemical modification of wood, nanoindentation provides the unique opportunity to investigate the relative contributions of cell wall property modification to the bulk property change.

Summary

The relation of nanoindentation to macroindentation is much different for wood than for other material systems because of the hierarchical structure of wood. The two indentation techniques resulted in deformation volumes that contain different structure and different dominant deformation mechanisms; thus, a direct comparison in hardness values was

inappropriate. However, we considered that nanoindentation may be used to investigate cell wall resistance to deformation, which then can be related to at least one of the deformation mechanisms in macroindentation (i.e., cell wall deformation of cellular structure). Comparisons between untreated and treated radiata pine samples demonstrated that nanoindentation can offer a new approach for investigating cell wall chemical modification mechanisms and their relative contributions to bulk wood properties.

References

ASTM. 2005. Annual book of standards, Vol. 04.10. Wood. American Society for Testing and Materials, West Conshohocken, PA. D143-94. Standard methods of testing small clear specimens of timber.

Bergander, A., and S. Salmen. 2002. Cell wall properties and their effects on the mechanical properties of fibers. J. Mater. Sci. 37:151-156.

Doyle, J., and J.C.F. Walker. 1985. Indentation hardness of wood. Wood Fiber Science. 17(3):369-376.

Ferranti L. Jr., R.W. Armstrong, and N.N. Thadhani. 2004. Elastic/plastic deformation behavior in a continuous ball indentation test. Mat. Sci. Eng. A 371:251-255.

Gindl, W., H.S. Gupta, and C. Grünwald. 2002. Lignification of spruce tracheids secondary cell walls related to longitudinal hardness and modulus of elasticity using nano-indentation. Can. J. Bot. 80(10): 1029-1033.

Gindl W., and H.S. Gupta. 2002. Cell-wall hardness and Young's modulus of melamine-modified spruce wood by nano-indentation. Composites: Part A 33(8):1121-1145.

Gindl W., and A. Teischinger. 2002. Axial compression strength of Norway spruce related to structural variability and lignin content. Composites: Part A 33: 1623-1628.

Gindl, W., and T. Schoberl. 2004. The significance of the elastic modulus of wood cell walls obtained from nanoindentation measurements. Composites Part A 35(12): 1345-1349.

Gindl, W., T. Schoberl, and G. Jeronimidis. 2004. The interphase in phenol-formaldehyde and polymeric methylene diphenyl-di-isocyanate glue lines in wood. Inter. J. Adhesion and Adhesives 24(4):279-286.

Gindl, W., H.S. Gupta, T. Schoberl, H.D. Lichtenegger, and P. Fratzl. 2004. Mechanical properties of spruce wood cell walls by nanoindentation. Appl. Phys. A 79:2069-2073.

Green, D., M. Begel, and W. Nelson. 2006. Janka hardness using nonstandard specimens, Res. Note FPL-RN-0303. U.S. Department of Agriculture, Forest Service, Forest Products Laboratory, Madison, WI.

Hirata, S., M. Ohta, and Y. Honma. 2001. Hardness distribution on wood surface. J. Wood Sci. 47:1-7.

Hofstetter, K., C. Hellmich, and J. Eberhrdsteiner. 2005. Development and experimental validation of a continuum micromechanics model for the elasticity of wood. European Journal of Mechanics A/Solids 24:1030-1053.

Holmberg, H. 2000. Influence of grain angle on Brinell hardness of Scots Pine (*Pinus sylvsetris* L.). Holz als Roh-und Werkstoff. 58:91-95.

Ibach, R.E., and W.D. Ellis. 2005. Chapter 15: Lumen Modifications, Handbook of Wood Chemistry and Wood Composites: edited by Roger M. Rowell, CRC Press, New York.

Jakes, J.E., D.S. Stone, and C.R. Frihart. 2007. Nanoindentation size effects in wood. In the proceedings of the 30th annual meeting of the adhesion society. Tampa Bay, FL, February 18-21. 15-17.

Jakes, J.E.. 2007. A proposed method for accounting for edge effects and structural compliance in nanoindentation of wood. M.S. Thesis. University of Wisconsin-Madison.

Jang, B.-K., and H. Matsubara. 2005. Hardness and Young's modulus of nanoporous EB-PVD YSZ coating by nanoindentation. J. Alloys Compounds 402:237-241.

Kelloge, R.M., C.B.R. Sastry, and R.W. Wellwood. 1975. Relationships between cell wall composition and cell wall density. Wood Fiber 7: 170-177.

Kelsey, K. 1963. A Critical review of the relationship between the shrinkage and structure of wood. CISRO Aust., Div. For. Prod. Tech. Paper No. 28.

Khor, K.A., L.G. Yu, O. Andersen, and G. Stephani. 2003. Effect of spark plasma sintering (SPS) on the microstructure and mechanical properties of randomly packed hollow sphere (RHS) cell wall. Mater. Sci. Eng. A 356:130-135.

Lakes, R. 1993. Materials with structural hierarchy. Nature 361:511-515.

Manika, I., and J. Maniks. 2006. Size effects in micro-and nanoscale indentation. Acta Materialia 54:2049-2056.

Moon, R.J., C. R. Frihart, and T. Wegner. 2006. Nanotechnology applications in the forest products industry. Forest Products Journal 56(5):4-10.

Neagu, R.C., E.K. Gamstedt, S.L. Bardage, and M. Lindstrom. 2006. Ultrastructural features affecting mechanical properties of wood fibres. Wood Material Science and Engineering. 1(3-4):146-170.

Pang, S. 2002. Predicting anisotropic shrinkage of softwood Part 1: Theories. Wood Sci. Tech. 36:75-91.

Sakai, M., and Y. Nakano. 2002. Elastoplastic load-depth hysteresis in pyramidal indentation. *Journal of Materials Research* 17(8):2161-2173.

Tze, W.T.Y, S. Wang, T.G. Rials, G.M. Pharr, and S.S. Kelley. 2007. Nanoindentation of wood cell walls: Continuous stiffness and hardness measurements. Composites: Part A 38:945-953.

Wimmer, R., B.N. Lucas, T.Y. Tsui, and W.C. Oliver. 1997. Longitudinal hardness and young's modulus of spruce tracheid secondary walls using nanoindentation techniques. Wood Sci Technol. 31:131-141.

Advanced Biomass Science and Technology for Bio-Based Products

Editors
Chung-Yun Hse, Zehui Jiang, and Mon-Lin Kuo

Associate Editors
Feng Fu and Paul Y. Burns

Developed from a symposium sponsored by:
Chinese Academy of Forestry & USDA Forest Service, Southern Research Station

May 23-25,2007
Beijing, China

Printed in the People's Republic of China.